IEEE Access
Multidisciplinary | Rapid Review | Open Access Journal

Received February 14, 2019, accepted February 22, 2019, date of publication February 27, 2019, date of current version March 20, 2019.

Digital Object Identifier 10.1109/ACCESS.2019.2902013

Research on Decoupling Problem of Suspension Gap and Location of Relative Position Sensor in High Speed Maglev Train

CHUNHUI DAI, GUIBIN LUO, AND ZHIQIANG LONG
College of Intelligence Science and Technology, National University of Defense Technology, Changsha 410073, China
Corresponding author: Chunhui Dai (daichunhui@maglev.cn)

This work was supported by the National Key R&D Program of China under Grant 2016YFB1200602.

ABSTRACT The relative position sensor of a high-speed maglev train is an important part of train location and speed detection for motor traction, but its output signal is not only related to position but also related to the suspension gap of the maglev train. The fluctuation of the suspension gap will affect the amplitude of the output signal of the sensor (i.e., the suspension wave signal is coupled with the output signal). The prediction normalization method currently used can eliminate the effect of the suspension fluctuation to a certain extent, but there is a limitation. Aiming at this problem, this paper analyzes the frequency characteristics of the suspension gap fluctuation caused by track irregularities and proposes a gap estimation algorithm based on the adaptive filter. The Kalman filter is used to estimate the gap and then the output signal is compensated according to the numerical relationship between the gap and the output signal of the sensor, so as to achieve the decoupling between the gap and the position measurement. Finally, the effectiveness of the method is proved by the comparison experiments.

INDEX TERMS High speed maglev train, relative position sensor, adaptive filter, Kalman filter, normalization.

I. INTRODUCTION

Relative position sensor is an important part of location and speed measuring system for high-speed maglev train. The direction, speed, cogging count and pole phase angle information of the train are all measured by relative position sensor [1], [2]. According to the description in [3], the relative position sensors are installed at the end of the two terminals of the maglev train, and the two is one set, which are mounted on one side. The detection probe of the relative position sensor is oriented to the long stator slot, and the positional relation between the installation position and the long stator is shown in Figure 1.

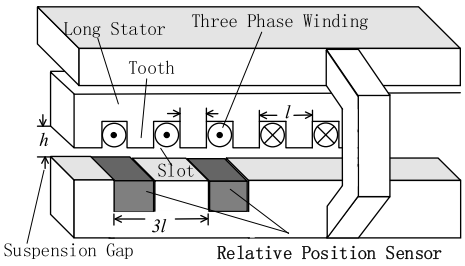

FIGURE 1. The installation diagram of relative position sensors.

The length of a cogging structure for the long stator is l, which is 86mm. The length of the tooth is l_w, which is 43mm, just half the cogging structure. The three windings of the traction linear motor are embedded in the slot [4]. Due to the alignment of the sensor probe and the suspension electromagnet, the distance between the sensor and the long stator is equal to the levitation gap, as the suspension works normally, usually 10mm. The long stator is made of superimposed silicon steel with magnetic conductivity, and the traction three-phase windings are multi-core aluminum cable. The magnetic permeability of aluminum is approximately 1. For the magnetic field, it is equivalent to the air (the permeability of the air is 1). The permeability of the silicon steel is as high as 7000∼10000, which is a good conductor of the magnetic field. When the sensor approaches to the long stator, the magnetic field excited by the detection coil in the probe will inevitably be affected by the superimposed silicon steel

The associate editor coordinating the review of this manuscript and approving it for publication was Mohammad Zia Ur Rahman.

in the long stator, leading to the change of the coil flux and the equivalent inductance of the coil. Therefore, this relationship can be used to detect the cogging structure of the long stator and to measure the position, which is basic principle of the relative position sensor.

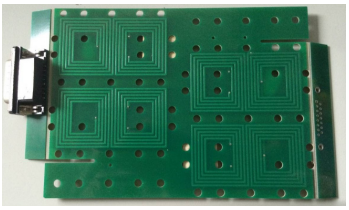

FIGURE 2. The coils in the probe of the sensor.

The electromagnetic environment below the bogie of the maglev train is complex. As the sensor is kind of electronic equipment, it is easy to be affected by electromagnetic field interference. As mentioned in [5], the sensor adopts the design of "8" word difference coils to reduce EMI, shown in Figure 2. This paper focuses on the influence of suspension gap.

II. INFLUENCE OF THE SUSPENSION GAP ON THE SENSOR

By the introduction of the principle of the sensor, it could be found that the output signal of the sensor depends on the change of the coil inductance. The inductance is not only related to the position of the horizontal direction relative to the cogging, but also to the distance vertical to the stator, namely the suspension gap [3]. During the running of the maglev train, the suspension gap is constantly fluctuating near the standard gap. When the maglev train is in static floating, the suspension gap has little change, and it has little influence on the sensor. When the train is running at a low speed, the disturbance of the track beam will cause fluctuation to the suspension system due to the geometric irregularity of the track beam and have a great influence on the sensor. The fluctuation of the suspension gap caused by track irregularity is shown in Figure 3.

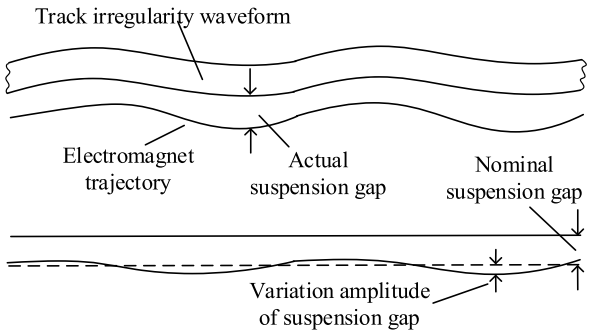

FIGURE 3. Schematic diagram of suspension gap fluctuation.

We need to find a way to make the sensor have the ability to decouple the position measurement and the suspension gap. Normally, the standard distance between the sensor probe and the stator plane is 10mm. As the sensor moves in the horizontal direction under the condition of constant speed, due to the periodicity of the long stator cogging, the inductance of the coil in the probe also changes periodically [5].

The aim of the relative position sensor is to detect the displacement in the horizontal direction, but the change of the suspension gap will affect the signal amplitude of the final output. The reason is that the high frequency magnetic field produced by the coil would attenuates in its normal direction. When the distance between the sensor and the long stator surface changes, the magnetization of the stator and the eddy current effect of the traction winding are also different. Therefore, the inductance changes of the coil are different in different suspension gaps. The inductance of the sensor coil and the waveform of the demodulation signals are shown in Figure 4 and Figure 5.

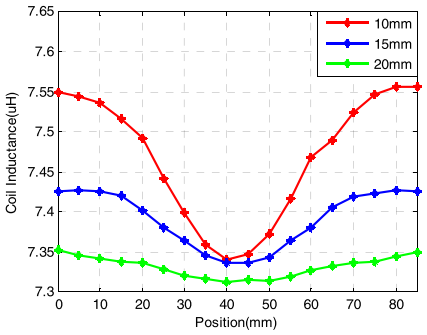

FIGURE 4. Waveforms of the coil inductance in one cogging cycle under different suspension gaps.

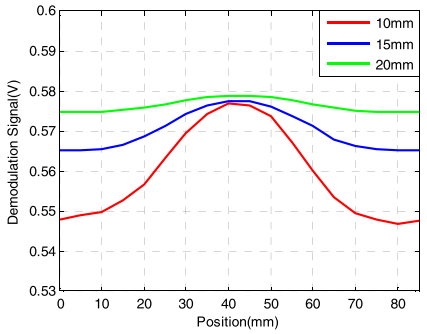

FIGURE 5. Waveforms of demodulation signals of one coil under different suspension gaps.

By the analysis of the detection circuit, it can be found that the resonant signal output from the coil is the amplitude modulation wave with constant frequency. The harmonic amplitude is only related to the coil inductance, and the equivalent inductance of the coil is related to the position of the horizontal cogging and the suspension gap. It can be concluded that the amplitude of the resonant signal is the function of two-variables, position x of the cogging structure and the suspension gap h, which can be expressed as:

$$f(t) = A(h, x)\cos(\omega t), \quad (0 < t \leq T) \tag{1}$$

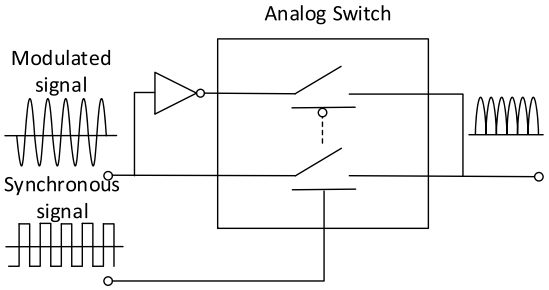

FIGURE 6. Synchronous detection mode based on analog switch.

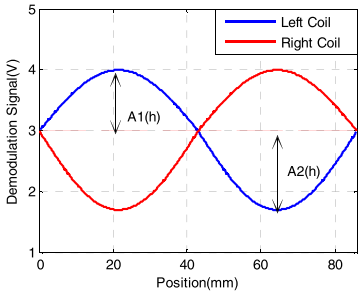

FIGURE 7. Demodulation signals of the left and the right coils.

We use a demodulation circuit based on analog switch, shown in Figure 6. According to the principle of synchronization demodulation, the demodulation amplitude is $2A(h, x)/\pi$.

When the gap is constant, the peak resonance value is a single-variable function of the position x. The probe is located at the top of the slot, the peak value is maximum, while at the top of the tooth, the peak value is the smallest, as shown in Figure 7. At any height, the above conclusions are all set up, and it can be expressed as:

$$\begin{cases} A_1(h) = A(h, x_t) \\ A_2(h) = A(h, x_s) \end{cases} \tag{2}$$

where x_t is the position of the tooth, and x_s is the position of the slot.

Reference [5] shows as the position changes, the demodulated voltage signal produces a periodic change with the long stator, which represents the position signal. The two resonant coils are symmetrical, forming a group and the width is just equal to the cogging structure. When the left coil is on the tooth, the right one is just on the slot. The conclusion can be drawn from Figure 7 that the demodulation signal and the cogging position are approximated as piecewise sinusoidal functions, which can be expressed as:

$$U_1(h, x) = \begin{cases} A_0(h) + A_1(h)\sin(2\pi\dfrac{x}{l}), & (0 < x \le \dfrac{l}{2}) \\ A_0(h) - A_2(h)\sin(2\pi\dfrac{x}{l}), & (\dfrac{l}{2} < x \le l) \end{cases}$$
$$U_2(h, x) = \begin{cases} A_0(h) - A_2(h)\sin(2\pi\dfrac{x}{l}), & (0 < x \le \dfrac{l}{2}) \\ A_0(h) + A_1(h)\sin(2\pi\dfrac{x}{l}), & (\dfrac{l}{2} < x \le l) \end{cases} \tag{3}$$

In the above formula, the sine amplitude $A_1(h)$ and $A_2(h)$ are the functions about the suspension gap and $A_0(h)$ is the bias function about suspension gap.

The output signal of the sensor can be obtained by subtracting the signals from the left and right, that is:

$$\begin{aligned} U(h, x) &= U_1(h, x) - U_2(h, x) \\ &= [A_1(h) + A_2(h)]\sin(2\pi\frac{x}{l}), \quad (0 < x \le l) \end{aligned} \tag{4}$$

Because $A_1(h)$ and $A_2(h)$ are all functions on the gap, the above formula can also be written as:

$$U(h, x) = M(h)\sin(2\pi\frac{x}{L}) \tag{5}$$

Among them, $M(h) = A_1(h) + A_2(h)$. According to the above formula, it can be concluded that the suspension gap and the position in the output signals are coupled.

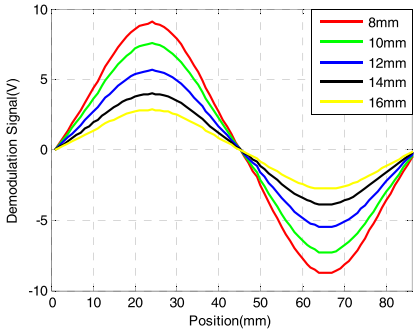

FIGURE 8. Output signals of the sensor under different suspension gaps.

By the finite element simulation, we can get the waveforms of the output signals under different suspension gaps, as shown in Figure 8.When the gap is reduced, the peak value of the signal is increased, and when the gap increases, the peak value decreases. Therefore, according to the relationship between the output signal amplitude and the suspension gap, we can get their numerical relationship by look-up table or linear interpolation, so as to reduce the influence of the levitation gap on the position measurement, which is the main content of this paper.

III. ANALYSIS OF FLUCTUATION AND FREQUENCY CHARACTERISCTIC OF SUSPENSION GAP

The positioning system of high speed maglev train provides the accurate magnetic pole phase for traction system only at low speed. When the train runs at a high speed, the positioning system does not provide. So it is necessary to analyse the frequency characteristics of the suspension gap at low speed.

The fluctuation of the suspension gap of the high speed maglev train is mainly due to the short wave irregularity of the track and the random interference of the external force [6]. The track irregularity mainly includes the following aspects:

(1) Installation error of the track stator surface, which is a kind of random error. The track of high speed maglev train is made of long stators with the length of 1032mm. The longitudinal and skew errors are inevitable when the stators

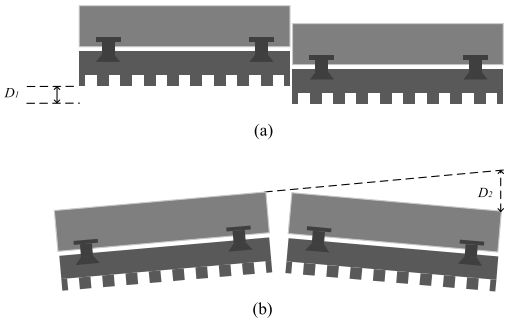

FIGURE 9. Installation errors of stators.

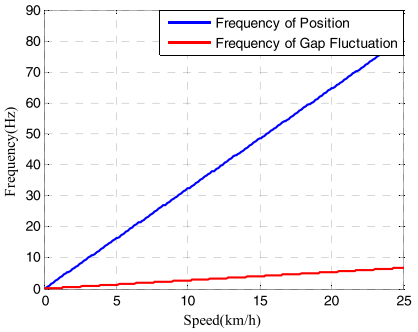

FIGURE 10. The relationship among the frequency of the position, the frequency of the suspension gap fluctuation and the speed.

are installed. As shown in Figure 9(a), D_1 is the longitudinal error in the stator. On the rampway, the track uses "the straight line replace" technology, so there exists a fitting error. In Figure 9(b), D_2 is a skew error between the adjacent stators.

(2)There are many curved and ramp sections in the maglev track, which are usually hundreds of meters in length. At the low speed, they have no effect on the suspension gap.

Reference [7] shows that the air gap signals were analyzed using short-time Fourier transform (STFT), which is used to determine the sinusoidal frequency and phase content of local sections of a signal as it changes over time. To determine the cause of stable composition, the excitation wavelength causing a change in frequency composition was analyzed. The relationship between these two parameters is given as:

$$f = \frac{v}{\lambda} \tag{6}$$

In the formula, λ is the track irregularity wavelength, f is the frequency, and v is the running speed of the train. We can find the frequency of the disturbance of the suspension gap at a certain speed at different wavelengths. Table 1 is the frequency of the suspension gap fluctuation corresponding to the different wavelengths when the train is running at the speed of 25km/h [7].

TABLE 1. The relationship between the wavelength and the frequency of the suspension gap.

Frequency(Hz)	Wavelength(m)	Causes
0.14-0.28	25-50	Irregularity of installation error track beams and functional parts, subgrade subsidence and other reasons.
6.7	1.032	Irregularity caused by longitudinal and skew installation errors of stator.

The frequency of the position signal is only related to the speed of the train. Its frequency range covers all the speed segments, and the signal wavelength is equal to the cogging length i.e.86mm. According the formula(6), the frequency is proportional to the speed, the speed range is 0∼25km/h, and the frequency range is 0∼80.7Hz.

As shown in Figure 10, the frequencies of the position signal and the gap fluctuation is overlapped on the spectrum throughout the range of the speed, which directly leads to that the filter with fixed filter cut-off frequency can not filter the AC components in the position dependent signal. However, we can see that, at a fixed speed, the two frequencies do not overlap on the spectrum, so the low-pass filter can be used to achieve the separation of the two signals.

At the low speed stage, the frequencies of the position signal and the suspension fluctuation is very low and close. At the stage of target stopping or traction starting, the speed of the train is often very low, but the precision of the pole phase angle is very accurate, i.e.8.6mm. Because of these problems, we need to propose a filter algorithm which can automatically adapt to each speed range with variable parameters.

IV. METHOD OF ELIMINATING THE INFLUENCE OF THE SUSPENSION GAP ON POSITION MEASUREENT

A. METHOD OF PREDICTION OF NORMALIZATION

The prediction normalization method is a simple and practical algorithm, which is used to eliminate the influence of the fluctuation of the suspension gap [8]. The method is used to normalize the output signal of the current period by measuring the amplitude of the output signal of the last period. Normalization transforms the current signal to that in the standard suspension gap, and the pole phase angle is calculated by look-up table. This method can be expressed as:

$$U(h, x) = \frac{M_s}{M(h_{n-1})} M(h_n) \sin(2\pi \frac{x}{L}) \tag{7}$$

M_s is the output signal amplitude of the sensor in standard suspension gap. $M(h_{n-1})$ is the output signal amplitude of the last period. $M(h_n)$ is the output signal amplitude of current period.

The prediction normalization method is based on the assumption that the suspension gap is invariable between the adjacent cogging when the train is running normally. The width of the cogging structure is only 86mm, so the time it takes for the train to pass through adjacent cogging is very short. The fluctuation frequency of the suspension gap is very low, so most of time, this assumption is set up. That is, the equation $M(h_{n-1}) = M(h_n)$ is established. After the

normalization process, the output signal of the sensor is as follows:

$$U(x) = M_s \sin(2\pi \frac{x}{L}) \tag{8}$$

The output signal is equal to that in the standard gap, which is independent of the suspension gap, and the accurate pole phase angle can be obtained through look-up table. However the premise of the assumption is that the suspension gap of the maglev train is unchanged between adjacent cogging. At low speed the suspension gap is sometimes changed, especially in the case of large installation error of the stators. So we designed a new method.

B. DECOUPLING METHOD BASED ON SUSPENSION GAP ESTIMATION

According to the principle of the sensor demodulation, the signals of the left and the right channels in the formula (3) are added, and we can obtain the sum signal:

$$\begin{aligned} U_h(h,x) &= U_1(h,x) + U_2(h,x) \\ &= 2A_0(h) + [A_1(h) - A_2(h)]\sin(2\pi \frac{x}{l}), \\ &\quad \times (nl < t \leq nl + \frac{l}{2}) \end{aligned} \tag{9}$$

In formula (9), the DC component (No change with x) $2A_0(h)$ in $U_h(h,x)$ is only related to the suspension gap and independent of the position, but the AC(Change with x) term is related to both of them. So measuring the addition of demodulation signals is impossible to accurately calculate the suspension gap.

If the AC component in the signals is filtered through filtering, the DC signal only related to the gap can be obtained. If the relationship between the amplitude of the DC signal and the gap is monotonous, the accurate functional relationship can be obtained by numerical calibration or curve fitting. In this way, the suspension gap can be calculated by real-time measurement of the DC component of the demodulation signal. If we get the relationship between the suspension gap and the output signal amplitude of the sensor, we can compensate for the output signal with suspension fluctuation, thus eliminating the influence of the change of the gap on the position detection [9].

Adaptive Filter (AF) can automatically adjust the internal parameters according to the change of the external environment. It consists of the two main parts: variable parameter filter and adaptive control law [10]. The adaptive control law is to adjust the parameters of the filter according to certain rules, so that the output of the filter converges to the optimal target. The structure is shown in Figure 11 [11]. In this paper, the purpose of the filter is to deal with AC components related to the relative position in the output signal of the sensor. Therefore, only the DC signal related to the suspension gap is left, and the suspension gap at the present time can be calculated through their relationship.

In the last section, the frequency characteristics of the position and the suspension gap have been analyzed. At any

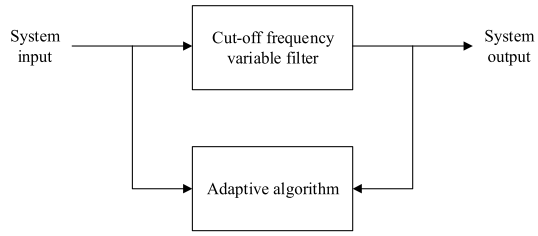

FIGURE 11. Structure of AF.

speed, the frequency of the position signal and the fluctuation frequency are not overlapped on the spectrum. The position signal is a relatively high frequency component, and the fluctuation signal is the component with low frequency. Only in the low speed range their frequencies are close, and the speed increases, the frequency distribution becomes wider. So only a low pass filter with variable cut-off frequency can be used to extract the suspension gap signal.

The finite impulse response (FIR) filter is a common digital filter, which has the advantages of simple structure and implementing easily in hardware and software. The FIR filter is always stable, and the function of low pass, high pass and band-pass can be realized through the design of parameters. The direct FIR filter is expressed as:

$$y(n) = \sum_{k=0}^{M-1} h(k)x(n-k) \tag{10}$$

The output of the FIR filter is a weighted linear combination of the inputs, and the actual structure is shown in Figure 12. It requires M-1 storage units to store M-1 inputs, each of which needs M multiplications and a M-1 additions [12].

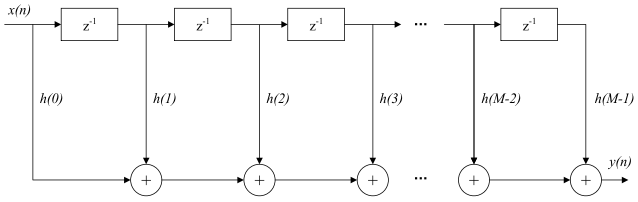

FIGURE 12. Implementation of the direct FIR filter.

The common methods for solving the FIR filter coefficient are window function method, frequency sampling method and so on. The window function method is suitable for the computer solution, so it is used so solve the low pass FIR filter coefficient of the specified cut-off frequency.

The expected low pass filter frequency response is shown as:

$$H_d(\omega) = \begin{cases} e^{-j\omega(M-1)/2}, & 0 \leq \omega \leq \omega_c \\ 0, & \text{others} \end{cases} \tag{11}$$

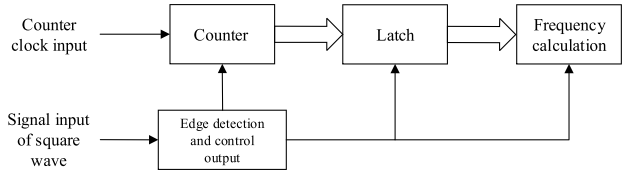

FIGURE 13. The structure of the digital frequency discriminator.

The corresponding unit impulse response can be expressed as:

$$h_d(n) = \frac{1}{2\pi}\int_{-\omega_c}^{\omega_c} e^{j\omega(n-\frac{M-1}{2})}d\omega = \frac{\sin[\omega_c(n-\frac{M-1}{2})]}{\pi(n-\frac{M-1}{2})}, \quad (n \neq \frac{M-1}{2}) \tag{12}$$

The Blackman window is selected as the window function, and the expression of the Blackman window function is as follows:

$$w(n) = 0.42 - 0.5\cos(\frac{2\pi n}{M-1}) + 0.08\cos(\frac{4\pi n}{M-1}), \times(0 \leq n \leq M-1) \tag{13}$$

By multiplying $h_d(n)$ with the Blackman window sequence in the upper form the FIR filter with the length of M of the unit pulse response can be obtained:

$$h(n) = \begin{cases} h_d(n)w(n), & 0 \leq n \leq M-1,\ n \neq \frac{M-1}{2} \\ \frac{\omega_c}{\pi}, & n = \frac{M-1}{2} \end{cases} \tag{14}$$

According to the formula (4) and formula (9), it is found that the frequency of the AC component in the sum signal is the same as that of the position signal. Therefore, the cut-off frequency of the FIR filter can be determined by measuring the frequency of the sensor output signal. The output signal of the sensor is approximately a sinusoidal signal, which can be turned into a square wave signal with the same frequency as the original signal by the hysteresis comparison. A digital frequency discriminator can be used, which can measure the frequency of the square wave. The structure of the discriminator is shown in Figure 13.

The edge detection and control output module controls the latch and reset of the counter value by detecting the rising or descending edge of the square wave [13]. When the rising edge of the square is coming, the high speed counter stops timing and latches the count to the output latch. Then the counter starts from zero. The frequency calculation module reads the value of the count latch, and the frequency of the square is as follows:

$$f = \frac{f_{clk}}{N} \tag{15}$$

N is the value of the count latch, and f_{clk} is the clock frequency of the counter.

C. SUSPENSION GAP ESTIMATION BASED ON KALMAN FILTER

Kalman filter (KF) provides a real-time, iterative method for filtering noisy data, which has been applied to various fields from aerospace to industry. The Kalman filter is an optimal estimation algorithm based on the linear state space model, which can filter the Gauss white noise contained in the system state [14], [15]. Due to the random size joints between the stators, there is a random noise interference in the frequency detection of the square, which directly affects the cut-off frequency of FIR low-pass filter and make the calculated suspension gap with noise.

The numerical relationship between the sum signal shown in formula (9) and the suspension gap can be measured by means of experiment. As shown in Figure 14, the diagram shows the waveforms of the sum signal under different gaps.

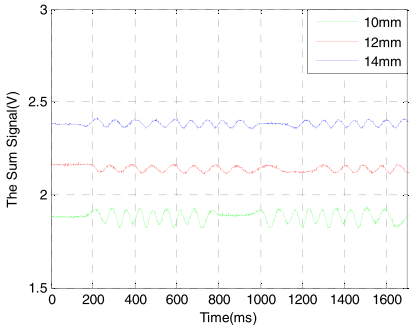

FIGURE 14. The sum signal with the information of suspension and position.

The sum signal after FIR processing is shown in Figure 15. Most of the AC component is filtered out, and there is DC signal associated with the suspension gap.

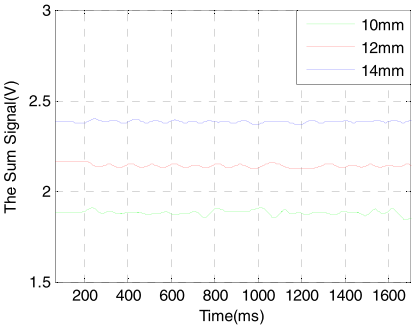

FIGURE 15. The sum signal after FIR processing.

It can be seen from Figure 15 that the relationship between the suspension gap and the filtered output signal is approximately linear, and the expression between the gap and the signal can be obtained by polynomial fitting method. The number of polynomial fitting n=1, the result is shown in Figure 16, and the formula is as shown:

$$g(h) = 0.015h + 0.295 \tag{16}$$

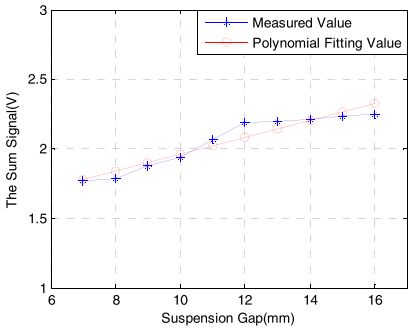

FIGURE 16. The fitting relationship between the output signal and the gap.

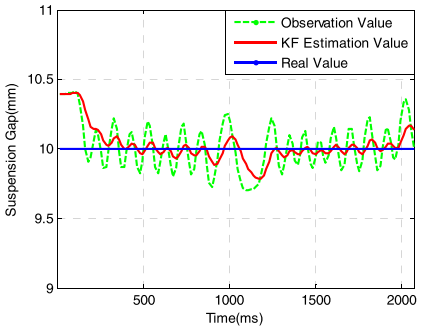

FIGURE 17. Comparison of the gap estimation after direct observation and KF.

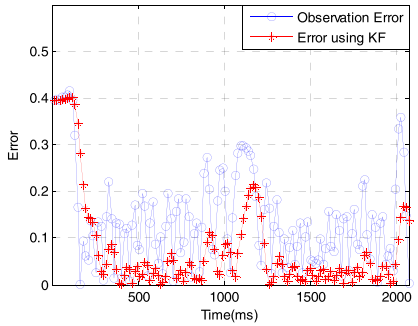

FIGURE 18. Analysis of gap estimation error.

The current gap can be calculated by formula (16). However, due to the stator joint and other reasons, there is still interference in the gap signal after AF process. In order to estimate the gap more accurately, KF is applied to the above liner model.

The state-space model of the gap estimation is as follows:

$$\begin{cases} X(k+1) = X(k) \\ Y(k) = 0.015X(k) + 0.295 \end{cases} \tag{17}$$

The Kalman filtering process of the above model can be described as the following steps:

(1)One step prediction of the state:

$$\hat{X}(k+1|k) = \hat{X}(k|k) \tag{18}$$

(2)One step prediction of covariance matrix:

$$P(k+1|k) = P(k|k) + Q \tag{19}$$

(3)Update of Kalman gain matrix

$$K(k+1) = P(k+1|k)(P(k+1|k) + R)^{-1} \tag{20}$$

(4)Update of covariance matrix

$$P(k+1|k+1) = (I - K(k+1))P(k+1|k) \tag{21}$$

(5)Update of state:

$$\begin{cases} \varepsilon(k+1) = Y(k+1) - [0.015\widehat{X}(k+1|k) + 0.295] \\ \widehat{X}(k+1|k+1) = \widehat{X}(k+1|k) + K(k+1)\varepsilon(k+1) \end{cases} \tag{22}$$

In the above process, Q is the covariance, R is the observed covariance, K(k+1) is the Kalman gain of next time, and $\widehat{X}(k+1|k+1)$ is the estimated value of the state at next time.

As shown in Figure 17, the estimated value of the gap after KF is closer to the real value than the direct observation. The estimation errors of the two methods are compared in Figure 18, and the observation errors of the Kalman filter are obviously less.

D. SUSPENSION GAP COMPENSATION FOR THE RELATIVE POSITION SENSOR

According to the analysis of the above sections, the block diagram of the position measurement and the suspension gap decoupling algorithm based on the AF, as shown in Figure 19, can be obtained. Firstly, the sensor demodulates the signal by subtraction operation on the differential output signal, which is coupled with small gap information. Secondly, the demodulation signals of the two coils of the sensor are added to get the sum signal containing the information of the gap and position, where the DC component corresponds to the gap signal, and the AC component corresponds to the position signal. Thirdly, the frequency characteristics of the position and the gap signal are analyzed, and AF algorithm is used to deal with the sum signal, and the suspension gap is obtained. In order to filter the random noise in the gap, the Kalman filter is used to estimate the real gap.

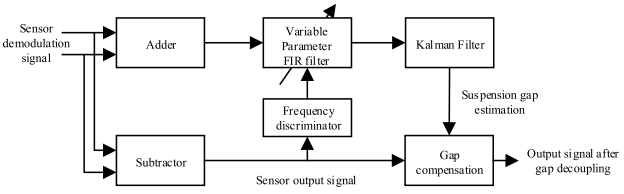

FIGURE 19. Block diagram of gap decoupling algorithm.

The output of AF algorithm is the real-time suspension gap of the maglev train and it can compensate the output

signal of the sensor. After compensation, the output is the position signal that removes the influence of the suspension gap. Then the position look-up table is carried out with the compensated position signal to obtain the pole phase angle. The compensated signal is expressed as:

$$U(h,x) = \frac{M_s}{M(h_n)} M(h_n) \sin(2\pi \frac{x}{L}) = M_s \sin(2\pi \frac{x}{L}) \quad (23)$$

M_s is the output amplitude of the sensor under the standard gap. $M(h_n)$ is the current output amplitude. Compared with the prediction normalization method, AF based on decoupling algorithm uses the real-time amplitude M_s instead of the amplitude of last time $M(h_{n-1})$. The latter can eliminate the influence of the gap better, and the real-time gap estimation is much more accurate.

V. CONCLUSION

When the suspension gap is constant and reduced, the output signal of the sensor is shown in Figure 20. It can be seen that when the gap is constant, the peak value of the signal is unchanged and the waveform is similar to the sine wave with equal amplitude. When the gap decreases, the amplitude of the signal increases because the distance between the probe and the cogging is reduced.

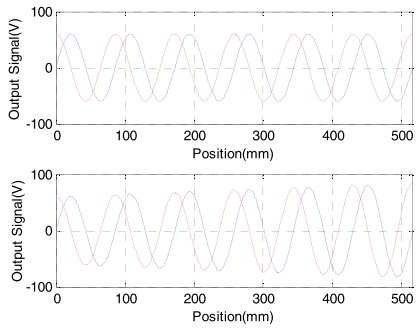

FIGURE 20. The output signal of the sensor.

The prediction normalization method, as is shown in Figure 21, can not completely eliminate the output signal error caused by the gap fluctuation.

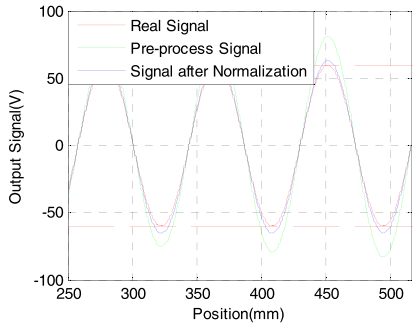

FIGURE 21. The dealt output signals using normalization method.

The suspension gap compensation algorithm based on AF is used to deal with the output signal of the sensor, and the results are shown in Figure 22.

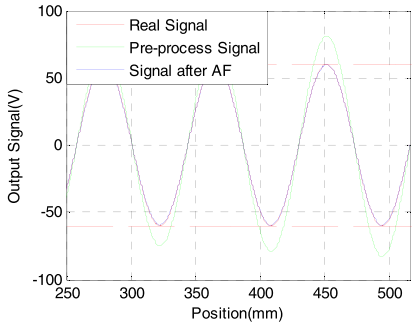

FIGURE 22. The dealt output signals using AF method.

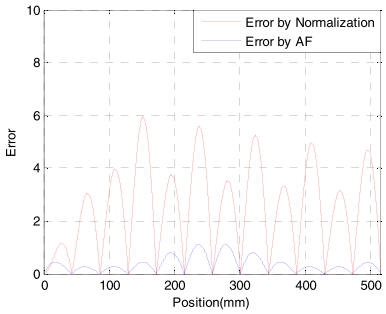

FIGURE 23. Error comparison between the two methods.

TABLE 2. Maximum statistical error at different heights.

Suspension Gap（mm）	Maximum error（mm）
2	4.15
4	2.72
10	1.43
20	2.15

From Figure 23, it is very intuitive to see that the error of gap compensation algorithm based on AF is smaller than that of prediction normalization method. The problem of normalization is that it is impossible to eliminate the influence of the gap fluctuation between the adjacent coggings. The adaptive method can compensate the position signal in real time so as to eliminate this kind of disturbance.

By converting the sampled voltage of the sensor to the actual position signal, the following error analysis table can be obtained by many field tests. The experimental results in Table II show that the proposed algorithm satisfies the requirement of position detection accuracy of traction (8.6mm) system at low speed.

ACKNOWLEDGMENT

Chunhui Dai and Prof. Zhiqiang Long contributed to the conception of the study. Chunhui Dai and Guibin Luo conceived and designed the experiments; Guibin Luo performed the experiments. Prof. Zhiqiang Long contributed significantly to analysis and manuscript preparation. Chunhui Dai wrote the paper. All the authors would like to thank the reviewers for their valuable work.

REFERENCES

[1] G. Wahl, "The maglev system transrapid—A future-oriented technology for track-bound transport systems," *Proc. Maglev*, 2004, pp. 32–36.
[2] H. C. Atzpodien, "Transrapid maglev system—Fields of application MAGLEV," in *Proc. 19th Int. Conf. Magnetically Levitated Syst. Linear Drives*. 2006.
[3] S. Xue, Z. Long, N. He, and W. Chang, "A high precision position sensor design and its signal processing algorithm for a maglev train," *Sensor*, vol. 12, no. 5, pp. 5225–5245, 2012.
[4] C. Dai, Z. Long, Y. Xie, and S. Xue, "Research on the filtering algorithm in speed and position detection of maglev trains," *Sensors*, vol. 11, no. 7, pp. 7204–7218, 2011.
[5] S. Xue, N. He, and Z. Long, "Electromagnetic field analysis and modeling of a relative position detection sensor for high speed maglev trains," *Sensors*, vol. 12, pp. 6447–6462, May 2012.
[6] F. Qin-hai, "Discussion on the demand of high-speed EMS vehicle on guide way irregularity," *China Railway Sci.*, vol. 23, no. 1, pp. 73–76, 2002.
[7] J. Shi *et al.*, "Measurements and analysis of track irregularities on high speed maglev lines," *J. Zhejiang Univ.-Sci. A*, vol. 15, no. 6, pp. 385–394, 2014.
[8] L. Lu, "The research on suspensive gap and relative position detecting technology in high speed maglev train," Ph.D. dissertation, School Nat. Univ. Defense Technol., Changsha, China, 2007.
[9] G. Luo, C. Dai, L. Tan, and Z. Long, "Research on suspension height and displacement decoupling of relative position detection sensor for high-speed maglev train," in *Proc. Int. Conf. Intell. Hum.-Mach. Syst. Cybern.*, 2017, pp. 346–350.
[10] S. Haykin, *Adaptive Filter Theory*. Upper Saddle River, NJ, USA: Prentice-Hall, 2002.
[11] Z.-Q. Long, A.-M. Hao, and W.-S. Chang, "Suspension controller design of maglev train considering the rail track periodical irregularity," *J. Nat. Univ. Defense Technol.*, vol. 25, no. 2, pp. 84–89, 2003.
[12] G. J. Proakis, *Digital Signal Processing Principle, Algorithms and Application*. Beijing, China: Electronics Industry, 2004.
[13] L. Wei, G. Ming, W. Hai-Hong, W. Qi, and S. Tie-Jiang, "ALL-digital discriminator by using a CPLD chip," *Laser Infrared*, vol. 32, no. 1, pp. 57–58, 2002.
[14] R. E. Kalman, "A new approach to linear filtering and prediction problems," *J. Basic Eng. Trans.*, vol. 82, no. 1, pp. 35–45, 1960.
[15] S. J. Julier and J. K. Uhlmann, "New extension of the Kalman filter to nonlinear systems," *Proc. SPIE*, vol. 3068, pp. 182–193, Jul. 1997.

Authors' photograph and biography not available at the time of publication.